NASA TECHNICAL TRANSLATION NASA TT F-14,120

ON THE OCCURRENCE OF LONGITUDINAL VORTICES IN TURBULENT BOUNDARY LAYERS AT CONCAVE WALLS

G. Sandmayr

Translation of: "Euber das auftreten von Laengswirbeln in Turbulenten Grenzschichten an Konkaven Waenden", Deutsche Luft-und Raumfahrt. DLR FB-66-41/June 1966 49 pages.

NATIONAL AERONAUTICS AND SPACE ADMINISTRATION
WASHINGTON, D. C. 20546 FEBRUARY 1972

ON THE OCCURRENCE OF LONGITUDINAL VORTICES IN TURBULENT BOUNDARY LAYERS AT CONCAVE WALLS

G. Sandmayr

ABSTRACT. The existence of periodic longitudinal vortices in a turbulent boundary layer along a concave wall is investigated. In addition to the velocity profile, a profile of the eddy viscosity and the Reynolds number are given. The eigenvalue problem is approximately solved for neutral disturbances and for a particular boundary layer by Galerkin's method, described by P. S. Klebanoff. The curve of critical curvature has a minimum for a certain wavelength of the disturbance. Within a certain range, it hardly changes with the Reynolds number. These results agree with experiments by I. Tani.

/4

1. INTRODUCTION

/7

In order to obtain some ideas on the origin of turbulence, there has often been interest in the stability of laminar boundary layers in relation to small perturbations compatible with the hydrodynamic equations of motion. At first there were studies of two-dimensional Tollmien-Schlichting waves propagating in the direction of flow. They received extensive theoretical and experimental study first in flows along plane walls and also, later, in flows along curved walls (see, for example, [1], Chapters XVI and XVII with extensive bibliographies).

Then, in 1940, H. Görtler introduced a relation for calculating the three-dimensional instability of laminar incompressible boundary layer flows at concave walls. It dealt with perturbations in the form of equidistant vortices having their axes in the direction of the basic flow [2]. G. I. Taylor [3] had previously demonstrated that similar vortices can originate in the flow between

two coaxially rotating cylinders, if the inner cylinder rotates faster than the outer one. The boundary layer flow mentioned above can be understood as a Taylor flow, in which the unperturbed outward flow takes the place of the internal rotating cylinder.

In a linearized theory, the law of vortex instability leads via the Navier-Stokes equations and the continuity equation, with consideration of the edge conditions for the perturbing quantities, to a three-parameter eigenvalue problem with the number $Re^2 \frac{\delta}{R}$, which still depends on the separation of the vortices and on a temporal regeneration factor, as the eigenvalue. Here δ is a measure of the boundary layer thickness; Re is the Reynolds number generated from δ and the outward flow; and R is the radius of curvature of the wall near which the flow passes $(\frac{\delta}{R} << 1)$. As in previous stability investigations, here too it is necessary to neglect changes in the basic flow and in the perturbing elements in the flow direction in order that the calculations can be performed. The basic flow is assumed to be steady.

For physical reasons, we are especially interested in the smallest positive eigenvalue of the problem. With neutral flows, i.e., those in which there is neither damping nor buildup, it forms, depending on the thickness of the vortex /8 assumed, a so-called critical curve, to which the following significance is ascribed: If the value $Re^2 \frac{\delta}{R}$ for a certain flow is below the critical value, then every perturbation of the type assumed will be damped. If it is above the critical value, then they can be built up, finally leading to turbulence.

The eigenvalue problem was approximately solved by H. Görtler. Following works supplemented the theory and refined the numerical treatment [4, 5, 6]. G. Hämmerlin [7] finally extended the stability investigations to laminar boundary layers in compressible media at different wall temperature relationships.

In this work we shall investigate the occurrence of longitudinal vortices in turbulent boundary layers. That is, if we consider turbulent flows which

may be divided into a time-averaged steady portion and nonsteady fluctuations, then the boundary layer theory can be applied to the time-average, with appropriate additional assumptions. Thus, it is obvious to ask whether longitudinal vortices can also be produced at concave walls by the interaction of centrifugal force, pressure, and viscosity forces.

Actually, I. Tani [21] in the experimental study of turbulent boundary layers at concave walls has established periodic fluctuations of the lines of constant velocity, which can be explained as resulting from the occurrence of longitudinal vortices. We shall compare the values obtained theoretically with the experimental results.

I thank Prof. Dr. H. Görtler for providing the impetus for this work. I would also like to thank Prof. Dr. E. Becker and especially Lecturer Dr. G. Hämmerlin for their active interest in the performance of this work, and for many valuable suggestions.

2. THE BASIC EQUATIONS OF TURBULENT FLOW

The nonsteady flow of an incompressible viscous fluid is described by the Navier-Stokes equations (see [8], Chapter IV, 2; or [1], Chapter III f)

$$\varrho \frac{D\mathfrak{w}}{Dt} = -\operatorname{grad} p + \operatorname{div} \mathfrak{T} \tag{2.1}$$

/9

and by the continuity equation

$$\operatorname{div} \mathfrak{w} = 0 \tag{2.2}$$

Here $\mathfrak{w}$ is the velocity vector of the flowing medium with components u, v, w in the directions of the orthogonal coordinates x, y, z; p is the pressure, ϱ the density, and $\mathfrak{T}$ the tensor of the friction stresses. $\mu = \mu(x,y,z)$ is the dynamic viscosity depending on the location. By div $\mathfrak{T}$ we mean the vector of divergence of the row vector of $\mathfrak{T}$. D/Dt symbolizes the hydrodynamic derivation with respect to time.

From (2.1), and considering (2.2), we obtain for an arbitrary orthogonal system the equations of motion

$$\rho\left\{\frac{\partial w}{\partial t} - w \times \operatorname{rot} w + \frac{1}{2}\operatorname{grad}(w^2)\right\} = \ldots \operatorname{grad} p$$

$$- \mu \operatorname{rot}(\operatorname{rot} w) + \operatorname{grad}\mu \times \operatorname{rot} w + 2\left\{(\operatorname{grad}\mu)\operatorname{grad}\right\} w \quad (1) \qquad (2.3)$$

or, in case μ = constant,

$$\rho\left\{\frac{\partial w}{\partial t} - w \times \operatorname{rot} w + \frac{1}{2}\operatorname{grad}(w^2)\right\}$$

$$= - \operatorname{grad} p - \mu \operatorname{rot}(\operatorname{rot} w) \,. \qquad (2.4)$$

To this we add the problem of the appropriate edge conditions.

In turbulent flow, the main movement has superimposed upon it an irregular fluctuating movement, so that the velocity and pressure are not constant at a fixed point in space. To represent the flow it is expedient to divide the instantaneous flow, according to O. Reynolds [9], into a time-steady portion averaged over a long period, and a nonsteady fluctuation. The fluctuation superimposed upon the main flow is so complex in detail that its theoretical calculation seems beyond hope. We shall limit ourselves to considering its effect on the average motion. That is, the mixed motion which it causes acts as if the viscosity were apparently very greatly increased. /10

If we designate the time-average values of the flow quantities as $\bar{u}$, $\bar{v}$, $\bar{w}$, $\bar{p}$, and the instantaneous deviations from them as u', v', w', and p', then for the actual velocities and pressure we have

$$w_i + \overline{w_i} = \overline{w_i} \quad \text{and} \quad p = \bar{p} + p' \,.$$

---

(1) The fact that the last summand is also independent of the coordinate system appears from the identity:

$$2\left\{(\operatorname{grad}\mu)\operatorname{grad}\right\} w = - \operatorname{rot}(\operatorname{grad}\mu \times w) + \operatorname{grad}\mu \operatorname{div} w - w \operatorname{div}(\operatorname{grad}\mu) + \operatorname{grad}\left\{(\operatorname{grad}\mu) w\right\} - \operatorname{grad}\mu \times \operatorname{rot} w - w \times \operatorname{rot}(\operatorname{grad}\mu)$$

As usual, the time-average is defined by

$$\bar{f}(x,y,z) = \frac{1}{2\tau} \int_{t_0-\tau}^{t_0+\tau} f(x,y,z,t)\, dt,$$

in which the time interval (1'1-) is chosen so large that $\bar{f}$ becomes independent of t_0 and τ. Further, the temporal limits should not depend on the location. Then differentiation and averaging are interchangeable.

We introduce the expansion of $\vec{w}$ and p into the equations of motion (2.4) and the continuity equation (2.2) and form the time average value by terms. Then all the linear expressions in the fluctuation magnitudes drop out, and we obtain

$$\rho\left\{-\bar{\vec{w}} \times \operatorname{rot}\bar{\vec{w}} + \frac{1}{2}\operatorname{grad}(\bar{\vec{w}}^2)\right\} = -\operatorname{grad}\bar{p} - \mu \operatorname{rot}(\operatorname{rot}\bar{\vec{w}}) + \rho\,\overline{\vec{w}' \times \operatorname{rot}\vec{w}'} - \frac{1}{2}\rho \operatorname{grad}(\overline{w'^2}) \qquad (2.5)$$

$$\operatorname{div}\bar{\vec{w}} = 0 \,. \qquad (2.6)$$

Because $\operatorname{div}\vec{w} = \operatorname{div}\bar{\vec{w}} + \operatorname{div}\vec{w}' = 0$ und $\operatorname{div}\bar{\vec{w}} = 0$ it also follows that $\operatorname{div}\vec{w}' = 0$. /11

If we subtract the term $\rho\,\overline{\vec{w}' \operatorname{div}\vec{w}'} = 0$ from the right side of Equation (2.5), all the expressions which affect the turbulent fluctuation motions can be combined into a vector, $\operatorname{div}\mathfrak{T}'$, where $\mathfrak{T}'$ is the symmetrical matrix

$$\mathfrak{T}' = -\rho \begin{pmatrix} \overline{u'^2} & \overline{u'v'} & \overline{u'w'} \\ \overline{u'v'} & \overline{v'^2} & \overline{v'w'} \\ \overline{u'w'} & \overline{v'w'} & \overline{w'^2} \end{pmatrix}$$

As we can see from comparison of Equation (2.5) with the Navier-Stokes equations (2.4) or (2.1), in the equation of motion for the time average we have added to the stress tensor of laminar friction, here designated $\bar{\mathfrak{T}}$, one more stress

tensor $\mathfrak{T}'$, the tensor of turbulent apparent viscosity. It was derived first by O. Reynolds [9] from the hydrodynamic equations of motion.

Edge conditions: All the components of $\bar{w}$ and w' vanish at solid walls. The fluctuation components are also very small near the wall. From this it follows that all the components of the tensor of turbulent apparent friction likewise vanish at solid walls, so that only the viscous stresses of laminar flow remain.

Calculation of the average motion from Equation (2.5) is possible only if the apparent stress of turbulent flow can be expressed by the values of the average motion, so that the differential equations contain only the average velocities and the average pressure. To achieve this, we assume, following I. Boussinesq [10] (cf. [11], page 124) that the mixed motion is simply equivalent to an enlargement of the viscosity effect, setting

$$\mathfrak{T}' = \frac{\varrho\varepsilon}{\mu}\bar{\mathfrak{T}}\,.$$

The quantity $\varrho\varepsilon$, which expresses the intensity of the mixed movement, corresponds to the viscosity parameter μ of the Stokes friction law. But the "apparent" kinematic viscosity ε is numerically much larger than the corresponding value ν of the laminar flow. We no longer are dealing with a material parameter. Instead, ε varies from case to case. In general, it depends on the spatial coordinates. In the individual case, it can only be decided experimentally how large the turbulent viscosity must actually be chosen. /12

In the case of simple, plane shear flow $\bar{u} = \bar{u}(y)$, $\bar{v} = \bar{w} = 0$, with $d\bar{u}/dy > 0$, which we shall take up later, we obtain approximate values due to the following considerations: Of the components of the tensor $\mathfrak{T}'$, there remains only the supplementary turbulent thrust stress

$$\tau_{xy}' = -\varrho\,\overline{u'v'} = \varrho\varepsilon\frac{d\bar{u}}{dy}$$

With this flow, the time average of the velocity fluctuations $\overline{u'v'}$ can be measured for any distance from the wall (see section 5); or, by means of various empirical laws, it can be linked with $\bar{u}(y)$ (e.g., the Prandtl mixing method formula, the von Karman similarity hypothesis; see [1], Chapter XIX). At any time, the apparent turbulent viscosity can be determined as a function of the wall distance from

$$\varepsilon(y) = -\frac{\overline{u'v'}}{d\bar{u}/dy}$$

For the total thrust stress of the flow, we can write

$$\tau_{xy} = \bar{\tau}_{xy} + \tau_{xy}' = (\mu + \varrho\,\varepsilon)\frac{d\bar{u}}{dy} = \mu_{eff}\frac{d\bar{u}}{dy}$$

in which the "effective" viscosity μ_{eff} is given by

$$\mu_{eff} = \mu - \varrho\,\frac{\overline{u'v'}}{d\bar{u}/dy} \tag{2.7}$$

(see [8], Chapter V, 9).

In the general case, too, we can formally combine the laminar viscosity μ and the turbulent apparent viscosity $\varrho\,\varepsilon$ into a quantity μ_{eff} and say: Boundary layer theory can be applied to the time-averaged value of the turbulent flow, if we take the fluctuation motions into account in the calculation by replacing the molecular viscosity by the much greater effective viscosity. /13

Corresponding to (2.3), then, the equations of motion for the average motion are

$$\begin{aligned}&\varrho\left\{\frac{\partial\bar{\vec{v}}}{\partial t} - \bar{\vec{v}}\times\operatorname{rot}\bar{\vec{v}} + \frac{1}{2}\operatorname{grad}(\bar{\vec{v}}^2)\right\}\\ &= -\operatorname{grad}\bar{p} - \mu_{eff}\cdot\operatorname{rot}(\operatorname{rot}\bar{\vec{v}}) + \operatorname{grad}\mu_{eff}\times\operatorname{rot}\bar{\vec{v}}\\ &+ 2\left\{(\operatorname{grad}\mu_{eff})\operatorname{grad}\right\}\bar{\vec{v}}.\end{aligned} \tag{2.8}$$

Because we are dealing here with a steady flow with $\bar{w} = \bar{w}(x,y,z)$, $\frac{\partial \bar{w}}{\partial t} = 0$. We shall keep the expression now so that we can later superimpose on it the non-steady perturbations.

3. THE COORDINATE SYSTEM

The following considerations are based on a coordinate system already used by G. Hämmerlin [7]. It is better suited to the flow conditions than the cylindrical coordinate system previously used in instability demonstrations of laminar flows. The usual approximations undertaken there in the boundary layer and extended to the exterior flow correspond to transition to a coordinate system in which the wall and all the coordinate lines (= flow lines) have the same constant curvature. In order to avoid error with this model, vortices of great thickness, which extend beyond the boundary layer, must be treated separately.

In the new system, we hypothesize that the segment of wall over which the flow passes, with constant radius of curvature R_0, is in the neighborhood of the valley of a wavy wall. The coordinate origin is placed at the point of the valley. We keep the assumption that the basic flow does not depend on the wall arc length. In this way, the amplitudes of the perturbing functions can later be taken as functions of the distance from the wall alone. Then the stability study leads to an eigenvalue problem in a system of ordinary differential equations. /14

As H. Görtler [12] has shown in an investigation of the laminar boundary layer at a wavy wall, the radius of curvature of the flow lines for $x = 0$ increases exponentially with increasing distance from the wall. In the vicinity of this line, therefore, it is reasonable to insert for the radius of curvature $R(y) = R_0 e^{ky}$, where y designates the perpendicular distance from the wall and the parameter k is still assumed to be given. Now we choose a family of coordinate lines of our system, so that it coincides with these flow lines.

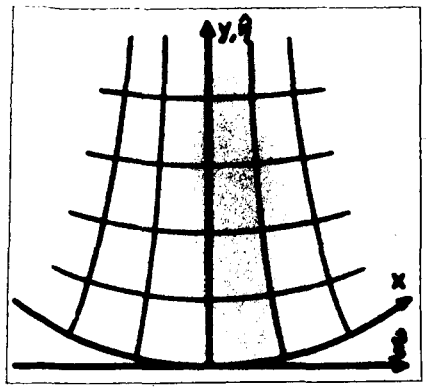

Figure 1. The coordinate system.

If we designate the Cartesian coordinates as $\hat{\xi}$, $\hat{\eta}$, $\hat{\zeta}$, and those of the new orthogonal system as x, y, z, then we obtain the following relation (see Appendix 1, page 35):

$$\hat{\xi} = x\, e^{\frac{-1}{kR_0}\,\frac{1}{kR(y)}}$$
$$\hat{\eta} = y$$
$$\hat{\zeta} = z\,.$$

In the line element $ds^2 = h_1^2 dx^2 + h_2^2 dy^2 + h_3^2 dz^2$,

$$h_1 = e^{\frac{-1}{kR_0}\,\frac{1}{kR(y)}}, \quad h_2 = h_3 = 1$$

and $$\frac{h_1'}{h_1} = -\frac{1}{R(y)} \text{ and } \left(\frac{h_1'}{h_1}\right)' = \frac{k}{R(y)}\,; \qquad ' = \frac{d}{dy}\,.$$

4. DERIVATION OF THE PERTURBATION DIFFERENTIAL EQUATIONS /15

In the coordinate form, the equations of motion (2.8) for turbulent flow (2.8) and the continuity equation (2.6) are

$$\rho\left\{\bar{u}_t + \frac{1}{h_1}\bar{u}\bar{u}_x + \bar{v}\bar{u}_y + \bar{w}\bar{u}_z + \frac{h_1'}{h_1}\bar{u}\bar{v}\right\} = -\frac{1}{h_1}\bar{p}_x$$
$$+ \mu_{eff}\left\{\bar{u}_{yy} + \bar{u}_{zz} + \left(\frac{h_1'}{h_1}\right)'\bar{u} + \frac{h_1'}{h_1}\bar{u}_y + \frac{h_1'}{h_1^2}\bar{v}_x - \frac{1}{h_1}\bar{v}_{xy} - \frac{1}{h_1}\bar{w}_{xz}\right\}$$
$$+ \frac{2}{h_1^2}(\mu_{eff})_x\left\{\bar{u}_x + h_1'\bar{v}\right\} + (\mu_{eff})_y\left\{\bar{u}_y - \frac{h_1'}{h_1}\bar{u} + \frac{1}{h_1}\bar{v}_x\right\}$$
$$+ (\mu_{eff})_z\left\{\bar{u}_z - \frac{1}{h_1}\bar{v}_x\right\}$$

$$\varrho\left\{\bar{v}_t + \frac{1}{h_1}\bar{u}\bar{v}_x + \bar{v}\bar{v}_y + \bar{w}\bar{v}_z - \frac{h_1'}{h_1}\bar{u}^2\right\} = -\bar{p}_y$$
$$+ \mu_{eff}\left\{\frac{1}{h_1^2}\bar{v}_{xx} + \bar{v}_{zz} - \frac{h_1'}{h_1^2}\bar{u}_x - \frac{1}{h_1}\bar{u}_{xy} - \bar{w}_{yz}\right\}$$
$$+ \frac{1}{h_1}(\mu_{eff})_x\left\{\frac{1}{h_1}\bar{v}_x - \frac{h_1'}{h_1}\bar{u} + \bar{u}_y\right\} + 2(\mu_{eff})_y\bar{v}_y$$
$$+ (\mu_{eff})_z\left\{\bar{v}_z + \bar{w}_y\right\}$$

$$\varrho\left\{\bar{w}_t + \frac{1}{h_1}\bar{u}\bar{w}_x + \bar{v}\bar{w}_y + \bar{w}\bar{w}_z\right\} = -\bar{p}_z + \mu_{eff}\left\{\frac{1}{h_1^2}\bar{w}_{xx} + \bar{w}_{yy}\right.$$
$$\left. + \frac{h_1'}{h_1}\bar{w}_y - \frac{1}{h_1}\bar{u}_{zx} - \frac{h_1'}{h_1}\bar{v}_z - \bar{v}_{zy}\right\} + \frac{1}{h_1}(\mu_{eff})_x\left\{\bar{u}_z + \frac{1}{h_1}\bar{w}_x\right\}$$
$$+ (\mu_{eff})_y\left\{\bar{v}_z + \bar{w}_y\right\} + 2(\mu_{eff})_z\bar{w}_z$$
$$\frac{1}{h_1}\bar{u}_x + \frac{h_1'}{h_1}\bar{v} + \bar{v}_y + \bar{w}_z = 0\,.$$

As we assume that changes of flow in the x-direction can be neglected, all derivatives with respect to x vanish from the equations. Now if we insert /16

$\frac{h_1'}{h_1} = -\frac{1}{R(y)}$ and $\left(\frac{h_1'}{h_1}\right)' = \frac{k}{R(y)}$ and transform the coefficients of μ_{eff} in the second and third equation of motion by means of the continuity equation, we obtain the differential equation system

$$\varrho\left\{\bar{u}_t + \bar{v}\bar{u}_y - \frac{1}{R(y)}\bar{u}\bar{v} + \bar{w}\bar{u}_z\right\} = \mu_{eff}\left\{\bar{u}_{yy} + \bar{u}_{zz}\right.$$
$$\left. + \frac{k}{R(y)}\bar{u} - \frac{1}{R(y)}\bar{u}_y\right\} + (\mu_{eff})_y\left\{\bar{u}_y + \frac{1}{R(y)}\bar{u}\right\} + (\mu_{eff})_z\bar{u}_z \qquad (4.1.1)$$

$$\varrho\left\{\bar{v}_t + \bar{v}\bar{v}_y + \bar{w}\bar{v}_z + \frac{1}{R(y)}\bar{u}^2\right\} = -\bar{p}_y + \mu_{eff}\left\{\bar{v}_{yy} + \bar{v}_{zz}\right.$$
$$\left. + \frac{k}{R(y)}\bar{v} - \frac{1}{R(y)}\bar{v}_y\right\} + 2(\mu_{eff})_y\bar{v}_y + (\mu_{eff})_z\left\{\bar{v}_z + \bar{w}_y\right\} \qquad (4.1.2)$$

$$\varrho\left\{\bar{w}_t + \bar{v}\bar{w}_y + \bar{w}\bar{w}_z\right\} = -\bar{p}_z + \mu_{eff}\left\{\bar{w}_{yy} + \bar{w}_{zz} - \frac{1}{R(y)}\bar{w}_y\right\}$$
$$+ (\mu_{eff})_y\left\{\bar{v}_z + \bar{w}_y\right\} + 2(\mu_{eff})_z\bar{w}_z \qquad (4.1.3)$$

$$-\frac{1}{R(y)}\bar{v} + \bar{v}_y + \bar{w}_z = 0 . \qquad (4.1.4)$$

As the basic flow, we choose a motion which is turbulent in the boundary layer, with a steady mean value which is assumed to depend only on the distance y from the wall. Let the time averages of the components $\bar{u}_0(y)$, $\bar{v}_0 = \bar{w}_0 = 0$, $\bar{P}_0(y)$ and $\mu_{eff}(y)$ be solutions of system (4.1).

So as to be able later to demonstrate the instability of this flow with respect to longitudinal vortices, we shall first derive the differential equations for small perturbations, which we superimpose on the basic flow in the following form:

$$\begin{aligned} \bar{u} &= \bar{u}_0(y) + u^*(y,z,t) \\ \bar{v} &= v^*(y,z,t) \\ \bar{w} &= w^*(y,z,t) \\ \bar{p} &= \bar{p}_0(y) + p^*(y,z,t) \\ \mu_{eff} &= \mu_{eff}(y) . \end{aligned}$$

In this first approximation we do not consider perturbations of the turbulent viscosity $\mu_{eff}(y)$, which can itself be calculated from averages of the fluctuation velocities. /17

Because of the assumption of small perturbations, we may linearize with respect to the starred values. The statement then leads to the differential equations

$$\varrho\left\{u_t^* + v^*\left(\frac{d\bar{u}_0}{dy} - \frac{\bar{u}_0}{R(y)}\right)\right\} = \mu_{eff}\left\{u_{yy}^* + u_{zz}^* + \frac{k}{R(y)}u^* - \frac{1}{R(y)}u_y^*\right\} + (\mu_{eff})_y\left\{u_y^* + \frac{u^*}{R(y)}\right\} \qquad (4.2.1)$$

$$\varrho\left\{v_t^* + \frac{2}{R(y)}\bar{u}_0 u^*\right\} = -p_y^* + \mu_{eff}\left\{v_{yy}^* + v_{zz}^* + \frac{k}{R(y)}v^* - \frac{1}{R(y)}v_y^*\right\} + 2(\mu_{eff})_y v_y^* \qquad (4.2.2)$$

$$\rho w_t^* = -p_z^* + \mu_{eff}\left[v_{yy}^* + v_{zz}^* - \frac{1}{R(y)} v_y^*\right] + (\mu_{eff})_y \left[v_z^* + w_y^*\right] \tag{4.2.3}$$

$$-\frac{1}{R(y)} v^* + v_y^* + w_z^* = 0 . \tag{4.2.4}$$

We add the conditions for adhesion to the wall and for decay of the perturbations for $y \to \infty$:

$$u^*(0,z,t) = v^*(0,z,t) = w^*(0,z,t) = 0$$

and

$$\lim_{y\to\infty} u^*(y,z,t) = \lim_{y\to\infty} v^*(y,z,t) = \lim_{y\to\infty} w^*(y,z,t) = 0 .$$

As can be shown later by means of the exact solution in the external region, the relation $\lim_{y \to \infty} p^*(y,z,t) = 0$ is also valid.

The assumption that $y << R(y)$ is justified for all values of y if we consider that $R_0 >> \delta$ (δ = boundary layer thickness) and if we accept the experimental value $k = 1/2\delta$[2] as the average value at a wavy wall. Then we have /18

$$R(y) = R_0 e^{ky} = R_0\left(1 + \frac{y}{2\delta} + \dots\right) >> y .$$

Following the deliberations in [2] and [4], because $\frac{1}{R(y)}|u_y^*| << |u_{yy}^*|$ and $\frac{1}{R(y)}|u^*| << |u_y^*|$, we neglect the terms on the left in these approximations because they are related to each other as $y/R(y)$ to 1. Further, it is true that $\frac{k}{R(y)}|u^*| << |u_{yy}^*|$. We proceed correspondingly for the other two velocity components.

---

[2] The value $k\,\delta = 1/2$ was previously used by G. Hämmerlin in the numerical calculations. It is taken from a work by H. Witting [13], in which the formation of vortices was investigated in the boundary layer along a wavy wall.

In (4.2.1) we may also neglect $\bar{u}_0/R(y)$ in relation to $d\bar{u}_0/dy$. The estimate is justified within the boundary layer. In the laminar external flow, we have

$$\left| \operatorname{rot} \bar{w}_0 \right| = \left| -\frac{d\bar{u}_0}{dy} + \frac{\bar{u}_0}{R(y)} \right| = 0 .$$

Now we consider special perturbations of the Taylor-Görtler vortex type, and set

$$\begin{aligned} u^*(y,z,t) &= u_1(y) \cos \alpha z \, e^{\beta t} \\ v^*(y,z,t) &= v_1(y) \cos \alpha z \, e^{\beta t} \\ w^*(y,z,t) &= w_1(y) \sin \alpha z \, e^{\beta t} \\ p^*(y,z,t) &= p_1(y) \cos \alpha z \, e^{\beta t} , \end{aligned}$$

in which $\alpha = 2\pi/\lambda$, λ = wavelength of the perturbation, and β = damping function constant.

Thus (with the primes indicating derivatives with respect to the argument y) system (4.2) transforms into

$$\varrho(\beta u_1 + v_1 \bar{u}_0') = \mu_{eff}(u_1'' - \alpha^2 u_1) + \mu'_{eff} u_1' \qquad (4.3.1)$$

$$\varrho\left(\beta v_1 + \frac{2}{R(y)} \bar{u}_0 u_1\right) = -p_1' + \mu_{eff}(-\alpha^2 v_1 + v_1'') + 2 \mu'_{eff} v_1' \qquad (4.3.2)$$

$$\varrho \beta w_1 = p_1 + \mu_{eff}(w_1'' - \alpha^2 w_1) + \mu'_{eff}(-\alpha v_1 + w_1') \qquad (4.3.3)$$

$$v_1' + \alpha w_1 = 0 . \qquad (4.3.4)$$

In treating this system, we shall first replace w_1 by v_1, according to (4.3.4). It would also be possible to eliminate $p_1(y)$, but then the second derivative of the turbulent viscosity $\mu_{eff}(y)$ would appear. As we shall see in Section 5, this profile cannot be given with sufficient accuracy. Thus we retain p_1 for the numerical calculations. /19

Now we introduce dimensionless quantities by

$$u = \frac{u_1}{u_\infty} \qquad M = \frac{\mu_{eff}}{\mu_\infty} \qquad \sigma = \alpha\delta$$

$$v = \frac{v_1}{u_\infty} \mathrm{Re} \qquad \bar{U} = \frac{\bar{u}_o}{u_\infty} \qquad \gamma = k\delta$$

$$p = \frac{p_1}{u_\infty^2} \mathrm{Re}^2 \qquad B = \frac{\delta^2 \varrho \beta}{\mu_\infty} \qquad \eta = \frac{y}{\delta}, \quad ' = \frac{d}{d\eta}$$

$$S = 2\,\mathrm{Re}^2 \frac{\delta}{R_o} \quad \text{mit} \quad \mathrm{Re} = \frac{\varrho u_\infty \delta}{\mu_\infty} .$$

Here u_∞ designates the velocity and μ_∞ the viscosity of the laminar external flow. Re is the Reynolds number formed with the external flow and the boundary layer thickness. Also, from the definition of μ_{eff} in (2.7) it is true that

$$M = \frac{\mu_{eff}}{\mu_\infty} = 1 - \frac{\varrho u_\infty \delta}{\mu_\infty} \frac{\overline{U'V'}}{d\bar{U}/d\eta} = 1 + \mathrm{Re}\, m(\eta) ,$$

if U', V' are fluctuation velocities of $\bar{U}(\eta)$ and $m(\eta)$ is a profile of the dimensionless kinematic viscosity, to be determined experimentally.

The value $\gamma = k\delta = 1/2$ is to be used in the numerical calculations. It matches the real conditions at a wavy wall*.

Now, the differential equations of the perturbing quantities u, v, p have the form

$$M(u'' - \sigma^2 u) + M'u' - Bu - v\bar{U}' = 0 \tag{4.4.1}$$

$$M(v'' - \sigma^2 v) + 2M'v' - Bv - S e^{-\gamma\eta} \bar{U} u - p' = 0 \tag{4.4.2}$$

$$M(v''' - \sigma^2 v') + M'(v'' + \sigma^2 v) - Bv' - \sigma^2 p = 0 . \tag{4.4.3}$$

*Translators Note: See footnote on page 12.

The edge conditions transform to

$$u = v = v' = 0 \quad \text{for} \quad \eta = 0 \quad \text{and} \quad \eta \to \infty \quad \text{and} \quad p(\infty) = 0 \,. \qquad /20$$

In the particularly important case of neutral perturbations, i.e., those which are neither built up nor damped, because B = 0, the system simplifies to

$$M(u'' - \sigma^2 u) + M'u' - v\bar{U}' = 0 \tag{4.5.1}$$

$$M(v'' - \sigma^2 v) + 2M'v' - S\, e^{-\gamma\eta}\, \bar{U}\, u - p' = 0 \tag{4.5.2}$$

$$M(v''' - \sigma^2 v') + M'(v'' + \sigma^2 v) - \sigma^2 p = 0 \tag{4.5.3}$$

$$u = v = v' = 0 \text{ for } \eta = 0 \text{ and } \eta \to \infty$$

or, if we neglect the difficulties in calculation of M'' and insert p from (4.5.3) into (4.5.2), to

$$M(u'' - \sigma^2 u) + M'u' - v\bar{U}' = 0 \tag{4.6.1}$$

$$M(v^{IV} - 2\sigma^2 v'' + \sigma^4 v) + 2M'(v''' - \sigma^2 v') + M''(v'' + \sigma^2 v) + \sigma^2 S\, e^{-\gamma\eta}\, \bar{U}\, u = 0 \,. \tag{4.6.2}$$

Thus the rule for vortex-like perturbations leads to an eigenvalue problem with the parameters Re, σ and δ/R_0. We can consider the number $S = 2\,Re^2\,\delta/R_0$ (Görtler parameter) as the eigenvalue. But, differing from previous studies with laminar flows, here the Reynolds number is already established by the choice of a particular viscosity profile.

The calculations which now follow to determine the smallest positive eigenvalue of the differential equation system (4.5) are to demonstrate the occurrence of longitudinal vortices at a concavely curved wall with

turbulent basic flow, and to provide, at least within an order of magnitude, information on the curvature at which a vortex of given wavelength can just be maintained, without decaying. For a fixed Reynolds number, then, the curve of critical curvature S or δ/R_0 can be calculated as a function of σ. Finally, we shall determine the effect of a change in the Reynolds number on these figures.

5. THE TURBULENT BASIC FLOW

/21

Before we can apply ourselves to the solution proper of the eigenvalue problem, we must obtain a profile $\bar{U}(\eta)$ for the time average velocity of turbulent basic flow along a weakly curved wall. The basic profile used in the following is taken from a work by P. S. Klebanoff ([18], Figure 3), in which he reports the results of measurements with longitudinal flow along a flat plate with zero pressure gradient. (The Reynolds number of the flow at the measuring point is given as $\frac{u_\infty x}{\nu_\infty} = 4{,}2 \cdot 10^6$ or $\frac{u_\infty \delta}{\nu_\infty} = 7{,}4 \cdot 10^4$). Because the curvature is weak, the flat plate is a usable approximation. In the work cited, we also find information on the distribution of the turbulent fluctuation velocities in the boundary layer. We will use them to derive a basic viscosity profile.

In relation to the numerical solution of the differential equation system, it was expedient to approximate the basic profile and its derivatives by polynomials. In order to cover the course of the curves well, we have divided them at appropriately selected points and defined the approximation polynomial in each of the intervals thus produced in such a way that the values of the functions and of the first derivatives agree at the junction points. By prescribing other functional values and derivative values at various supporting points within the intervals, we could in general achieve agreement between the curves prescribed graphically and the approximate curves described by the polynomials, within the presently possible accuracy of drawing. The approximating polynomials are listed separately in Appendix 2 (page 30).

Figure 2 shows the distribution of the average velocity $\bar{U}(\eta)$ in the boundary layer, according to P. S. Klebanoff, and the derivative of the velocity profile. The curve near the wall is plotted separately. As we can see from the diagram, the velocity profile of the turbulent boundary layer is characterized by a steep rise at the wall and a rather even course in the rest of the region. The derivative $\bar{U}'(\eta)$ was obtained by graphical differentiation of the basic profile.

Figure 3 shows the curve which Klebanoff ([18], Figure 5) called /22

$\frac{\overline{u'v'}}{u_\infty^2} = s(\eta)$ (u', v' fluctuation velocities). It describes the course of the entire thrust stress $\frac{\tau}{\rho u_\infty^2}$ of turbulent flow.

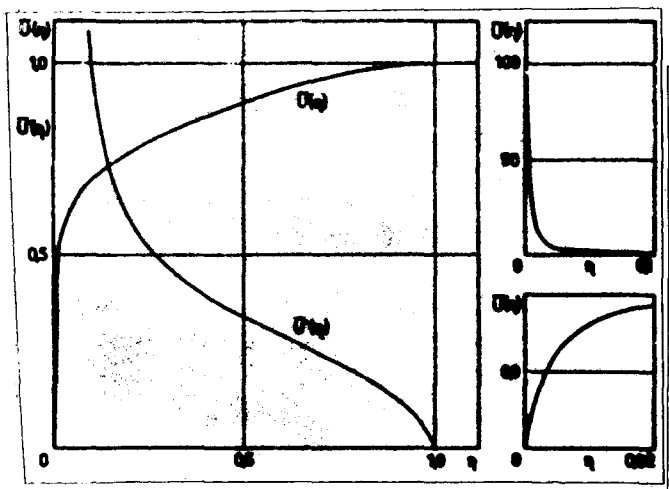

Figure 2

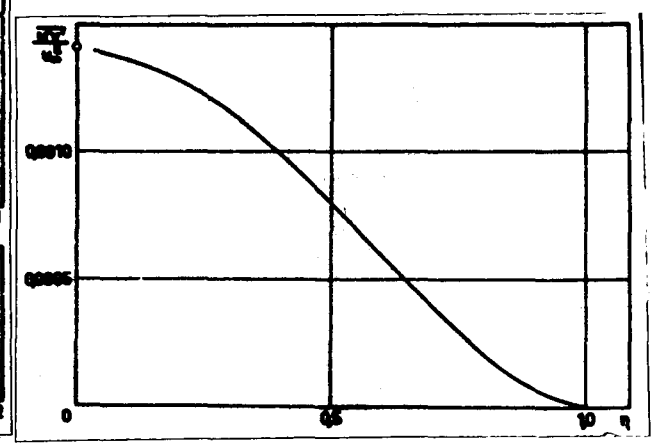

Figure 3

At the measuring point nearest the wall ($\eta = 0.035$) the frictional stress reached two percent of the total value.

The desired profile $m(\eta) = \frac{\overline{u'v'}/u_\infty^2}{d\bar{U}/d\eta} = \frac{\overline{U'V'}}{d\bar{U}/d\eta}$, which denotes the dimensionless turbulent apparent viscosity, was calculated point by point from the quotients of the approximation polynomial for the turbulent thrust stress /23 $s(\eta)$ and for the derivative of the basic profile. It is plotted with respect to η in Figure 4.

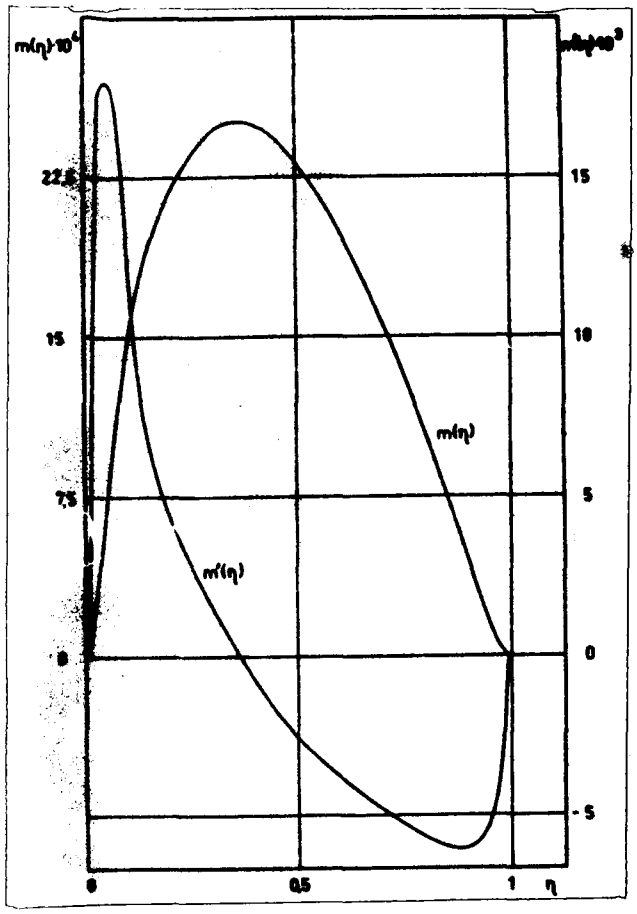

Figure 4. The dimensionless turbulent apparent viscosity and its derivative.

The curve was modified slightly in the intervals $0 \leq \eta \leq 0.1$ and $0.9 \leq \eta \leq 1$, so that the boundary conditions $m(0) = m'(0) = 0$ and $m(1) = m'(1) = 0$ are fulfilled. They correspond to the disappearance of the additional viscosity in the laminar underlayer and on transition into the external flow. The points of inflection, which must occur in the given intervals, could not be determined exactly. Thus the approximation of $m(\eta)$ in the boundary regions is quite inexact. For the approximation of $m'(\eta)$, essentially the derivatives of the approximation polynomial for $m(\eta)$ were used. $m''(\eta)$ can no longer be stated with reasonable accuracy. /24

6. SOLUTION METHODS

In the case where $M \equiv 1$, we have from (4.6), except for the factor $e^{-\gamma\eta}$ at S, the perturbation differential equations for a laminar incompressible boundary layer flow which have been treated often already. In [2] and [4] this system of differential equations is converted by means of Green functions into a system of integral equations. The principle of Jentzsch (see [4], page 290) then guarantees the existence of a simple, positive smallest eigenvalue with its eigenfunctions, which can be obtained by an iteration procedure given by H. Wielandt.

Because $M = M(\eta)$, and in the case of a turbulent boundary layer, this method corresponds to the transition from a differential equation system (4.5) to a system of integral and differential equations, with the added difficulty that derivatives of unknown quantities still occur in the integrands. The numerical effort is considerably greater here than in laminar boundary layers.

Because of the unfavorable form of the coefficients, the use of difference methods for numerical determination of the eigensolutions of the differential equation system involves great difficulties.

But, on the other hand, the differential equation system can be handled by means of approximation methods. R. C. di Prima [14, 15] and A. M. O. Smith [6] use the method of Galerkin [16, 17] in particular to determine the eigenvalues and eigenfunctions of similar systems of differential equations in hydrodynamic stability investigations. As this method has proved very effective in many cases, and because it is relatively simple to apply, we use it to derive a first approximate solution.

The method of Galerkin is described extensively in Appendix 3, so that we can limit ourselves to a brief explanation here. We start with the eigenvalue problem (4.5). In place of the dependent variables u, v, p, approximate solutions $\hat{u}$, $\hat{v}$, $\hat{p}$ are introduced into the differential equations. Here we are dealing with a linear combination of each of q linear independent functions, each of which fulfills its boundary conditions in detail. The Galerkin method consists only in determining the 3q constants of the starting set, so that now the expressions on the left side of (4.5) are orthogonal to certain starting functions in the integration interval $(0, \infty)$. To be sure, if the first expression is orthogonalized to all the starting functions for u, the second and third are correspondingly orthogonalized to those for v and p. Thus we obtain a system of 3q linear homogeneous equations. This can be written in matrix notation as $(\alpha + \hat{S}\beta)\, c = 0$. α and β are square matrices of 3q columns, and c is the column vector of the unknown constants. By means of the iteration

/25

method, we calculate the smallest positive eigenvalue $\hat{S}_1$ and its constants from the linear equation system. $\hat{S}_1$, and the functions $\hat{u}$, $\hat{v}$, $\hat{p}$ represent approximations to the smallest positive eigenvalue of (4.5) and its eigenfunctions.

The accuracy with which the eigensolutions of the differential equation system are approximated by the linear equation system depends essentially on the prescription of suitable starting functions. It can be improved further if the number of starting functions is increased, but this also increases the cost of the work and the errors in the numerical computation. The following considerations were decisive for the selection of the starting functions:

Because $\bar{U}(\eta) \equiv 1$ and $M(\eta) \equiv 1$, in the region $\eta \geq 1$, differential equations (4.5) simplify to

$$\begin{array}{lll} u'' - \sigma^2 u = 0 & u(\infty) = 0 \\ v'' - \sigma^2 v - p' - S\, e^{-\gamma\eta}\, u = 0 & v(\infty) = 0 \\ v''' - \sigma^2 v' - \sigma^2 p = 0 & v'(\infty) = 0 \end{array}$$

with the solutions (d_i = constant; i = 1, 2, 3)

$$u = d_1\, e^{-\sigma\eta} \tag{6.1.1}$$

$$v = (d_2 + d_3\eta)e^{-\sigma\eta} - \frac{d_1\sigma^2}{[(\sigma+\gamma)^2 - \sigma^2]^2}\, S\, e^{-(\sigma+\gamma)\eta} \tag{6.1.2}$$

$$p = 2d_3\, e^{-\sigma\eta} + \frac{(\sigma+\gamma)d_1}{(\sigma+\gamma)^2 - \sigma^2}\, S\, e^{-(\sigma+\gamma)\eta}. \tag{6.1.3}$$

/26

Thus as $\eta \to \infty$ all the eigenfunctions approach zero at least as rapidly as $e^{-\sigma\eta}$ or $\eta e^{-\sigma\eta}$. From (6.1.1) and the boundary condition $u(0) = 0$, it also follows that the continuous differentiable function $u(\eta)$ has at least one extreme in the interval $0 < \eta < 1$ and that the sign does not change for $\eta \geq 1$. Also, $v(\eta)$ has at least one extreme in the interval $0 < \eta < \infty$.

Functions of the form $h(\eta) = (1 - e^{-\eta})^n e^{-r\eta}$ with integral non-negative n and r show a similar course. As all the boundary conditions of (4.5) are also satisfied with satisfactory choice of the exponents, we can use linear combinations of such functions as approximate solutions.

7. RESULTS

First, approximate values $\hat{S}$ for the smallest eigenvalue of (4.5) were calculated by the method described in Section 6 and Appendix 4, with various combinations of two to ten starting functions each. With the parameter values $\sigma = 1$ and $Re = 7 \cdot 10^4$ maintained, the following results were obtained:

Depending on the combination of the starting functions used for the approximation, the eigenvalues and eigenfunctions varied for the same number q of starting functions. For q - 3 the eigenvalues are approximately in the range $7.5 \cdot 10^5 \leq \hat{S} \leq 2.3 \cdot 10^6$. With q = 4, the range of variation is somewhat smaller, and the eigenvalues lie within the limits $7 \cdot 10^5 \leq \hat{S} \leq 1.5 \cdot 10^6$. The differences, which are in part considerable, can be explained thus:

In the computation of the elements of the matrices $\boldsymbol{\alpha}$ and $\boldsymbol{\beta}$, there appear as integrands products of coefficient functions of the differential equation system with starting functions and their derivatives. As the coefficient functions $\bar{U}'(\eta)$, $M(\eta)$ and $M'(\eta)$ have distinct extremes in the interval [0, 1], the course of the integrand functions, and thus the value of the integrals, is strongly affected by the choice of the starting functions. But changes in the magnitude and signs of the matrix elements cause shifts in the eigenvalues. /27

If we add more starting functions to an already existing combination, we can observe no convergence of the solutions toward a difinite value. Rather, the eigenvalues with these approximations generally become somewhat smaller, while the eigenfunctions usually show greater fluctuations. Here it must

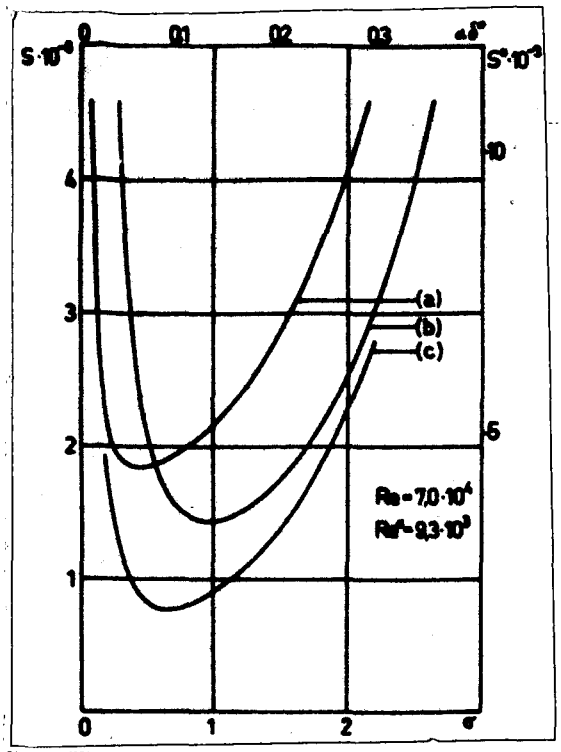

Figure 5. Approximations for the curve of the parameter $S = 2\,Re^2 \frac{\delta}{R}$.

certainly be considered that, with six or more starting functions, the errors which occur in the numerical treatment of the problem become significant. They can to some extent considerably falsify the rssult. As we can in any case except only an order-of-magnitude view of the solutions, we shall in the following be satisfied with a small number of starting functions.

Our next objective is to investigate the dependence of the parameter S on the wavelength σ of the prescribed perturbation. Three different typical approximations to the curve of critical curvature are plotted in Figure 5. Combinations of three to five starting functions were used to compute the balue $\hat{S}$. These closely approximate the appropriate eigenfunctions in the vicinity of the point $\sigma = 1$. Individually, they are (see Appendix 4 for the notations):

(a)

$$\hat{u}_{11} = (1-e^{-\eta})\, e^{-\eta}, \quad \hat{u}_{12} = (1-e^{-\eta})^2\, e^{-\eta}, \quad \hat{u}_{13} = (1-e^{-\eta})^3\, e^{-2\eta}$$

$$\hat{v}_{21} = (1-e^{-\eta})^2\, e^{-2\eta}, \quad \hat{v}_{22} = (1-e^{-\eta})^4\, e^{-2\eta}, \quad \hat{v}_{23} = (1-e^{-\eta})^6\, e^{-3\eta}$$

$$\hat{p}_{31} = e^{-\eta}, \quad \hat{p}_{32} = (1-e^{-\eta})^2\, e^{-\eta}, \quad \hat{p}_{33} = (1-e^{-\eta})^3\, e^{-2\eta}$$

(b)

$$\hat{u}_{1k} = (1-e^{-\eta})\, e^{-(k+1)\eta}$$

$$\hat{v}_{2k} = (1-e^{-\eta})^2\, e^{-(k+1)\eta} \qquad k = 1,2,3,4$$

$$\hat{p}_{31} = e^{-2\eta}, \quad \hat{p}_{3k} = (1-e^{-\eta})\, e^{-(k+1)\eta}, \qquad k = 2,3,4$$

(c)

like (b) with k = 1, 2, 3, 4, 5.

By means of the example solutions plotted in Figure 5, we can clarify the differences which can occur among the approximate values $\hat{S}$ found for a prescribed wave length σ. But it is a common characteristic of all of the curves $\hat{S}(\sigma)$ that they show a minimum for a definite σ, rising steeply for larger and smaller values of the parameter. We may assume that the exact solution also behaves in this way, and that there is a smallest critical curvature for a prescribed turbulent boundary layer flow. To be sure, we cannot make any exact statements on the position and value of the minimum on the basis of the approximations we have.

Figure 6 shows the curves for the eigenfunctions $\hat{u}(\eta)$ and $\hat{v}(\eta)$, which appear in the computation of S by means of the starting functions (a) and (b) for the parameter values $\sigma = 1$ and $Re = 7 \cdot 10^4$. In each case, Max $u(\eta) = 1$ and Max $| \hat{v}(\eta) | = 1$ were chosen for normalization. The eigenfunctions hardly change as long as σ is in the interval [0, 1;2]. /29

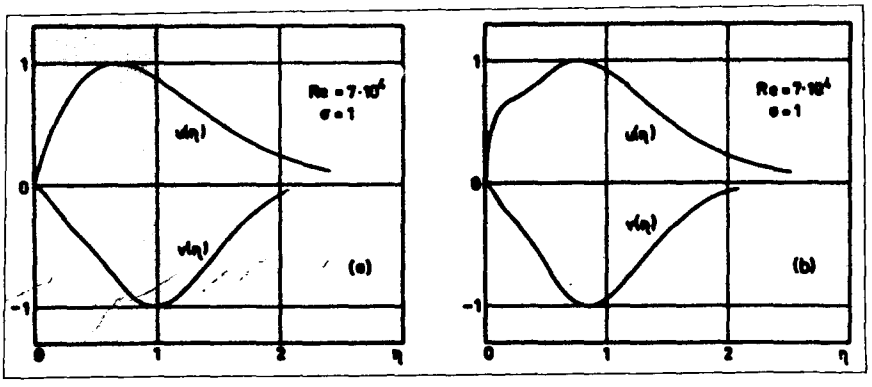

Figure 6. Approximations for the eigenfunctions $u(\eta)$ and $v(\eta)$.

In order to compare the curves of critical curvature at different Reynolds numbers, we refer all quantities to the displacement thickness δ^*

or to the pulse loss thickness ϑ ; both are physically reasonable measures of the boundary layer thickness.

The displacement thickness is defined by

$$\delta^* = \delta \int_0^1 [1 - \bar{u}(\eta)]\,d\eta \ ,$$

and the pulse loss thickness by

$$\vartheta = \delta \int_0^1 \bar{u}(\eta)\,[1 - \bar{u}(\eta)]\,d\eta \ .$$

For the basic profile from Section 5, we calculate $\delta^* = 0{,}1334\ \delta$ and $\vartheta = 0{,}0995\ \delta$. From this we immediately obtain $\delta^* = 1{,}342\ \vartheta$ or $\vartheta = 0{,}746\ \delta^*$. The Reynolds number formed with the displacement thickness is designated as Re*, and the value referred to the pulse loss thickness as Re_ϑ. Analogously, for the Gortler parameter, $S^* = 2\,Re^{*2}\frac{\delta^*}{R_o}$ and $S_\vartheta = 2\,Re_\vartheta^{\,2}\frac{\vartheta}{R_o}$.

J. Nikuradse ([19]; cf. [1], page 500) has shown that affine velocity profiles appear with turbulent plate flow in the range of Reynolds numbers $1{,}7 \cdot 10^6 \leq Re_x \leq 18 \cdot 10^6$ (x = path distance) if $\frac{\bar{u}}{u_\infty}$ is plotted vs. $\frac{y}{\delta^*}$. If the path length x is replaced by the boundary layer thickness by means of the conversion formula given in ([1], page 475)

/30

$$\delta(x) = 0{,}37\ (Re_x)^{-1/5}$$

then this applies correspondingly for the parameter value $3{,}6 \cdot 10^4 \leq Re \leq 2{,}4 \cdot 10^5$ and, according to the relation

$$\delta^*(x) = 0{,}1738\ (Re_x)^{-0{,}139}\ x$$

found in [19], for the Reynolds numbers $4 \cdot 10^3 \leq Re^* \leq 3 \cdot 10^4$. As J. Nikuradse ([20]; see [1], page 475) has also established in the study of turbulent tube flow, the dimensionless kinematic apparent viscosity plotted vs. the dimensionless wall distance very rapidly approaches a limiting curve with increasing Reynolds number. That is, with sufficiently large Reynolds number ($\gtrsim 10^5$) the turbulence mechanism no longer changes, and the turbulence is "saturated".

We assume that in turbulent boundary layer flow also the apparent kinematic viscosity $m(\eta)$ does not change significantly with the Reynolds number. Then if we vary the Reynolds number within the range as delimited above and refer the results to δ^*, we can use the profiles of $U(\eta)$ and $m(\eta)$ given in Section 5 to study the dependence of the curve of critical curvature on the Reynolds number.

Figure 7 shows the curve of the critical Gortler parameter S^* vs. $\alpha\delta^*$ for different values of the parameter Re^*. The starting functions (a) and (b) were used for approximation. As was to be expected, the curves of $(\alpha\delta^*)$ are shifted as a whole upward with increasing Reynolds number, while the abscissa of the minimum hardly changes.

If we plot instead the critical curvature $\frac{\delta^*}{R_0}$ formed from the displacement thickness at various Reynolds numbers vs. $\alpha\delta^*$, then it appears, as can be seen in Figure 8, that the curves differ only slightly from each other. To be sure, they are lower the larger the Reynolds number. /31

Finally, let us make a comparison with experimental results. I. Tani [21] has made velocity measurements in laminar and turbulent boundary layers along a concavely curved wall. In every case, he found that the lines of constant velocity have periodic fluctuations in the z-direction. The amplitude of these fluctuations becomes greater with increasing path length of the flow, while the wavelength hardly changes. These fluctuations could be explained as the result of a system of longitudinal vortices.

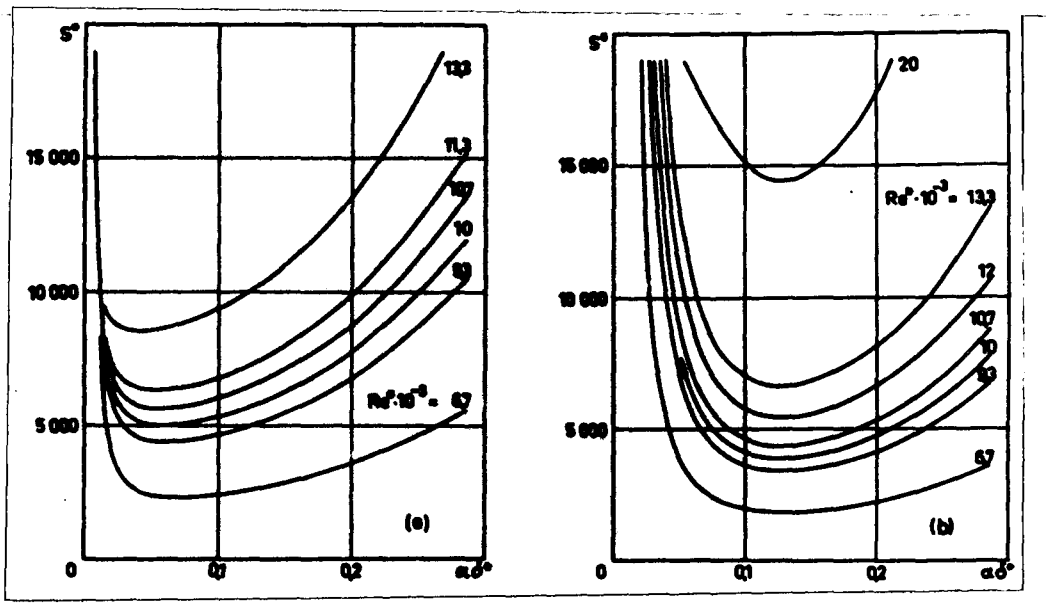

Figure 7. Curve of the critical Görtler parameter at various Reynolds numbers.

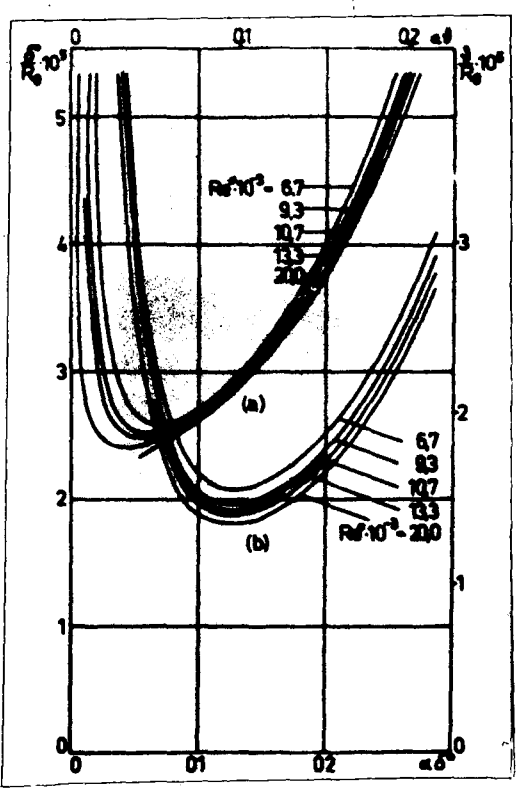

Figure 8. Curves of critical curvature for different Reynolds numbers.

In the laminar case, the results of I. Tani agree well with the values calculated in [2], [4], and [6]. But because he knew of no theoretical or experimental studies on whether longitudinal vortices could occur at concave walls even in turbulent boundary layers, he set up the following deliberations to find comparison values:

In laminar flows, the perturbations build up even at relatively small Reynolds numbers [6]; but certain turbulent flows behave like laminar ones [22] at a low Reynolds number which one can obtain by replacing the kinematic viscosity ν by the turbulent

viscosity ν_T. Furthermore, the studies in [2] and [4] have shown that a small change in the velocity profile has little effect on the curve of the Görtler parameter produced with the pulse loss thickness.

From this I. Tani concludes that the stability diagram given by A. M. O. Smith [6], which shows the parameter $G = \frac{u\vartheta}{\nu}\sqrt{\frac{\vartheta}{R_0}}$ as a function of $u\vartheta$, also applies for concavely curved boundary layers if ν is merely replaced by ν_T. Following F. H. Clauser [22] he used for this the approximation which is valid for the outer 80 - 90% of the boundary layer, $\nu_T = 0{,}018\, u\delta^*$. Then if he assumes, following [22], that $\delta^* = 1{,}3\,\vartheta$, the Reynolds number in G can be replaced by the number $\frac{1}{0.018 \cdot 1.3} = 43$, and the parameter for the turbulent boundary layer is $G_T = 43\sqrt{\frac{\vartheta}{R_0}}$. /33

The Clauser approximation $\nu_T = 0{,}018\, u\,\delta^*$ corresponds approximately to the maximum value of the effective viscosity calculated in Section 5. That is, if in

$$M(\eta) = \frac{\nu_{eff}(\eta)}{\nu_\infty} = 1 + m(\eta) \cdot \frac{\delta}{\delta^*} Re^*$$

with

$$\max_{0 \le \eta \le 1} m(\eta) = 0{,}0025 \quad \text{and} \quad \frac{\delta}{\delta^*} = 7{,}5$$

we neglect the contribution from laminar viscosity, then we have

$$\max_{0 \le \eta \le 1} \nu_{eff}(\eta) \approx 0{,}0025 \cdot 7{,}5\, u_\infty \delta^* = 0{,}0188\, u_\infty \delta^*$$

The solutions of (4.5) can better be compared with the critical curve of A. M. O. Smith if ν in G is replaced by an average value for the effective viscosity. As the average value of $m(\eta)$ we find $\bar{m} = 0.0016$. As above, with

this we obtain the mean effective viscosity $\bar{\nu}_{eff} \approx 0{,}016\, u_\infty \vartheta$. Then the parameter G corresponds to the value $G_\nu = 62\sqrt{\frac{\vartheta}{R_o}}$.

Figure 9 shows the neutral curve (1) of A. M. O. Smith [6] for laminar flows as well as the newly calculated critical curve for the incompressible case from G. Hämmerlin [7]. Curves (3) and (4) were obtained as approximate solutions with turbulent basic flow with the starting functions (a) and (b) for the parameter value $Re = 7 \cdot 10^4 (Re^* = 9{,}3 \cdot 10^3, Re_\vartheta = 7 \cdot 10^3)$. They are plotted as $(\alpha\vartheta, 43\sqrt{\frac{\vartheta}{R_o}})$- and $(\alpha\vartheta, 62\sqrt{\frac{\vartheta}{R_o}})$- diagrams.

The results of I. Tani's measurements at concavely curved walls with radii of curvature R_o = 5 m and R_o = 10 m are also plotted in Figure 9. With the radius of curvature of 5 m, a wavelength of about 6.5 cm was observed, and thus the wave number α = 1. With R_o = 10 m, it was estimated that α = 2.

For the log-log plot used in Figure 9, the measurements for vortices of constant wavelength lie on straight lines because of the identity $43\sqrt{\frac{\vartheta}{R_o}} \equiv \frac{43}{\sqrt{\alpha R_o}}\sqrt{\alpha\vartheta}$. As the wavelength of the vortex hardly depends on the incident flow velocity, these straight lines almost coincide at the same radii of curvature. /34

As was to be expected, the experimental values are significantly higher than the theoretically calculated curves of critical curvature. Here we must consider that I. Tani found a built-up vortex, while the theoretical considerations are based on neutral perturbations.

A1. The Coordinate System /35

The basic quantities of the orthogonal coordinate system introduced in Section 3 arise from the following deliberations:

In the Cartesian $\hat{\xi},\hat{\eta}$-system, the lines y = constant are described by

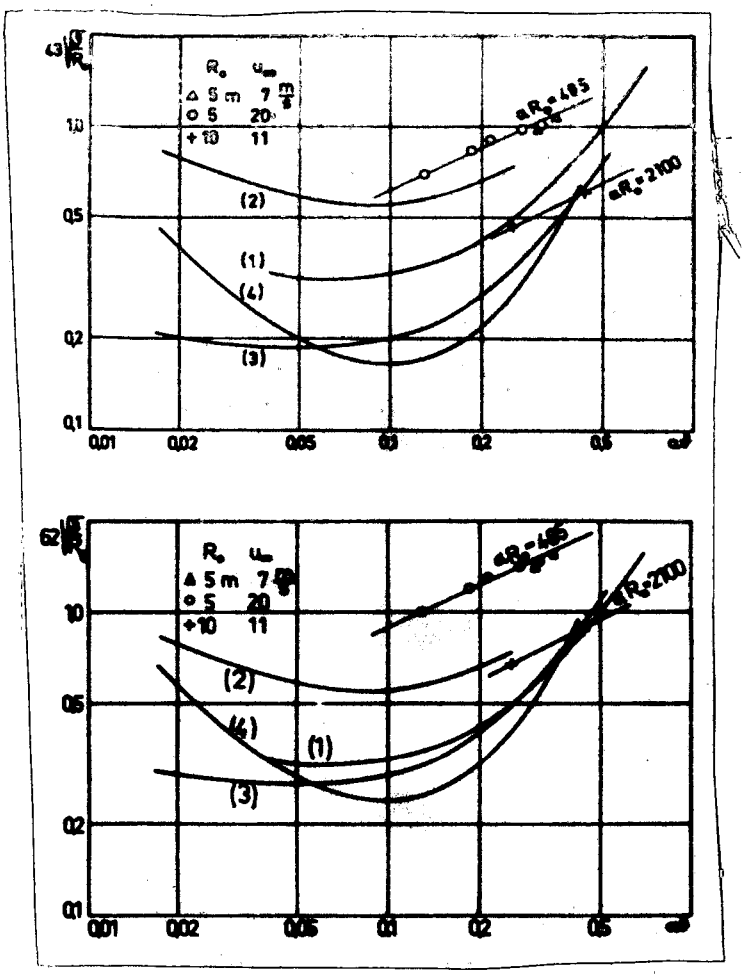

Figure 9. Comparison of the measurements of I. Tani with the theoretically calculated critical curves: (1) A. M. O. Smith [6]; (2) G. Hämmerlin [7]. Curves (3) and (4) were calculated with approximations (a) and (b).

$$\hat{\xi}^2 + [\hat{\eta} - \{R(y) + y\}]^2 = R(y)^2 \qquad \text{(A1.1)}$$

The differential equation for this family of curves is

$$\frac{d\hat{\eta}}{d\hat{\xi}} = \frac{-\hat{\xi}}{\hat{\eta}-(R+y)} \qquad \text{(A1.2)}$$

In order to eliminate the parameter y, we solve (A1.1) for $\hat{\eta}$:

$$\hat{\eta} = R(y) + y - \sqrt{R(y)^2 - \hat{\xi}^2}\ .$$

In the vicinity of the $\hat{\eta}$-axis, where the orthogonal grid is only defined, the estimate $\frac{\hat{\xi}^2}{R(y)^2} \ll 1$ applies, so that, approximately, $\hat{\eta} = y$.

The differential equation of the orthogonal family with the parameter x = constant now appears from (A1.2) to be

$$\frac{d\hat{\eta}}{d\hat{\xi}} = -\frac{R(\hat{\eta})}{\hat{\xi}}, \quad \text{and} \quad R(\hat{\eta}) = R_o\, e^{k\hat{\eta}};$$

and its general solution is

$$K(x)\,\hat{\xi} = e^{\frac{1}{k\,R(\hat{\eta})}}.$$

To determine K(x) we now set $\hat{\eta} = 0$, thus obtaining $K(x)\hat{\xi} = e^{\frac{1}{kR_o}}$. On the other hand, $x(\hat{\xi})$ is calculated as the arc length at the wall (y = 0) from

$$\frac{dx}{d\hat{\xi}} = \sqrt{1 + \left(\frac{d\hat{\eta}}{d\hat{\xi}}\right)^2} \quad \text{with} \quad \hat{\eta} = R_o - \sqrt{R_o^2 - \hat{\xi}^2}$$

giving /36

$$x(\hat{\xi}) = \int_0^{\hat{\xi}} \frac{R_o}{\sqrt{R_o^2 - t^2}}\, dt = R_o \arcsin \frac{\hat{\xi}}{R_o}.$$

Now it is approximately true that $\frac{\hat{\xi}}{R_o} \approx \sin\frac{x}{R_o} \approx \frac{x}{R_o}$, if only $\frac{x^2}{R_o^2} \ll 1$, so that we obtain $K(x) = \frac{1}{x} e^{\frac{1}{kR_o}}$.

Thus we obtain

$$\hat{\xi} = x \cdot e^{\frac{-1}{kR_o}} \cdot e^{\frac{1}{kR(y)}}$$
$$\hat{\eta} = y$$
$$\hat{\zeta} = z .$$

A2. Approximation Polynomial

a) Basic velocity profile

For $0 \le \eta \le 0{,}02$:

$$\bar{u}_1(\eta) = 104{,}964\ \eta - 8511{,}20\ \eta^2 + 333518\ \eta^3 - 5030864\ \eta^4 .$$

For $0{,}02 \le \eta \le 0{,}08$:

$$\bar{u}_2(\eta) = 0{,}45063 + 7{,}37708\ \eta - 121{,}677\ \eta^2 + 1147{,}71\ \eta^3 - 4289{,}49\ \eta^4 .$$

For $0{,}08 \le \eta \le 1$:

$$\bar{v}_3(\eta) = 0{,}54067 + 2{,}33040\,\eta - 10{,}5938\,\eta^2 + 33{,}2311\,\eta^3 - 61{,}6051\,\eta^4 + 65{,}7088\,\eta^5 - 37{,}3249\,\eta^6 + 8{,}71278\,\eta^7 .$$

For $\eta \geq 1$:

$$\bar{v}_4(\eta) = 1 .$$

b) Derivative of the basic velocity profile

For $0 \leq \eta \leq 0{,}02$:

$$\bar{v}_1'(\eta) = (0{,}105 - 20{,}0867\,\eta + 1657{,}76\,\eta^2 - 65138{,}9\,\eta^3 + 990556\,\eta^4) \cdot 10^3 .$$

For $0{,}02 \leq \eta \leq 0{,}08$:

$$\bar{v}_2'(\eta) = (0{,}026765 - 3{,}03591\,\eta + 165{,}6218\,\eta^2 - 5040{,}312\,\eta^3 + 90725{,}96\,\eta^4 - 9618260\,\eta^5 + 5557002\,\eta^6 - 13505490\,\eta^7) \cdot 10^3 .$$

/37

For $0{,}08 \leq \eta \leq 0{,}2$:

$$\bar{v}_3'(\eta) = 3{,}56967 - 53{,}6702\,\eta + 387{,}814\,\eta^2 - 1300{,}45\,\eta^3 + 1654{,}66\,\eta^4 .$$

For $0{,}2 \leq \eta \leq 1$:

$$\bar{v}_4'(\eta) = 1{,}34694 - 7{,}50079\,\eta + 30{,}3451\,\eta^2 - 82{,}3014\,\eta^3 + 148{,}4773\,\eta^4 - 169{,}8662\,\eta^5 + 109{,}3569\,\eta^6 - 29{,}8578\,\eta^7 .$$

For $\eta \geq 1$:

$$\bar{v}_5'(\eta) = 0 .$$

c) Thrust stress of the turbulent flow

For $\eta \leq 1$:

$$s(\eta) = (1{,}41 - 0{,}2308\,\eta - 1{,}9604\,\eta^2 - 1{,}0938\,\eta^3 + 2{,}1354\,\eta^4 - 0{,}2604\,\eta^5)\cdot 10^{-3}\ .$$

For $\eta \geq 1$:

$$s(\eta) = 0\ .$$

d) Dimensionless turbulent apparent viscosity

For $0 \leq \eta \leq 0{,}2$:

$$m_1(\eta) = 0{,}40835\,\eta^2 - 3{,}9185\,\eta^3 + 14{,}765\,\eta^4 - 20{,}150\,\eta^5\ .$$

For $0{,}2 \leq \eta \leq 0{,}95$:

$$m_2(\eta) = (0{,}345397 + 16{,}7883\,\eta - 64{,}0363\,\eta^2 + 198{,}474\,\eta^3 - 464{,}887\,\eta^4 + 637{,}583\,\eta^5 - 454{,}883\,\eta^6 + 130{,}567\,\eta^7)\cdot 10^{-3}.$$

For $0{,}95 \leq \eta \leq 1$:

$$m_3(\eta) = -4{,}3546 + 17{,}5412\,\eta - 26{,}4186\,\eta^2 + 17{,}632\,\eta^3 - 4{,}4\,\eta^4\ .$$

For $\eta \geq 1$:

$$m_4(\eta) = 0\ .$$

e) Derivative of the turbulent apparent viscosity /38

For $0 \leq \eta \leq 0{,}2$:

$$m_1'(\eta) = 0{,}82525\,\eta - 12{,}0374\,\eta^2 + 61{,}5380\,\eta^3 - 107{,}161\,\eta^4\ .$$

For $0{,}2 \leq \eta \leq 0{,}95$:

$$m_2'(\eta) = 0{,}0167883 - 0{,}1280725\,\eta + 0{,}595421\,\eta^2 - 1{,}859550\,\eta^3 + 3{,}187914\,\eta^4 - 2{,}729299\,\eta^5 + 0{,}913966\,\eta^6 .$$

For $0{,}95 \le \eta \le 1$:

$$m_3'(\eta) = 17{,}5412 - 52{,}8372\,\eta + 52{,}896\,\eta^2 - 17{,}6\,\eta^3 .$$

For $\eta \ge 1$:

$$m_4'(\eta) \equiv 0 .$$

A3. The Method of Galerkin

This section describes how the method of Galerkin [16, 17] is applied to determine eigenvalues and eigenfunctions for linear homogeneous differential equations with linear homogeneous boundary conditions. In order to explain the method, it is sufficient to consider a differential equation containing one independent parameter. Then, by obvious generalization, we obtain a rule for the treatment of differential equation systems.

Given a differential equation of n^{th} order

$$K[x] + S\,L[x] = 0 \qquad \text{(A3.1)}$$

with n linear homogeneous boundary conditions within an interval [a, b], with $x = x(t)$. Let S be the independent parameter and K, L be differential operators of the form

$$\sum_{\nu=1}^{n} f_\nu(t) \frac{d^\nu}{dt^\nu} \qquad \text{(A3.2)}$$

To determine an approximate solution of the eigenvalue problem, we first establish a function $\hat{x} = \hat{x}(t; c_1, c_2, \ldots, c_q)$ which for arbitrary values of the /39

independent constants $c_1, \ldots, c_q$ satisfies all the boundary conditions. If these are linear, as in the present case, then $\hat{x}$ can be chosen as a linear combination of q independent linear functions $\hat{X}_1, \ldots, \hat{X}_q$ which again satisfy the same boundary conditions:

$$\boxed{\hat{x} = \hat{X}\, c = \sum_{k=1}^{n} \hat{X}_k\, c_k} \qquad \text{(A3.3)}$$

with $\boxed{\hat{X} = (\hat{X}_1, \ldots, \hat{X}_q)}$ and $c' = (c_1, \ldots, c_q)$, where ' indicates a transposed matrix.

Let $\Delta(t)$ be the defect function which arises if the approximation $\hat{x}$ is inserted into the left side of (A3.1):

$$\boxed{K[\hat{x}] + S\, L\,[\hat{x}] = \Delta(t).}$$

For a good approximation, this defect should in a certain sense be the "smallest possible" in the entire interval. In order to achieve this, we follow Galerkin, selecting the independent constants $c_1, \ldots, c_q$ so that variously weighted means of the defects, integrated over the interval [a,b], vanish. As the multipliers, we can use the starting functions themselves (or the first q functions of a complete system). As the operators are linear, there arises in this way a system of q simultaneous linear homogeneous algebraic equations in the unknown constants $c_1, \ldots, c_q$, which can be written in matrix form as follows:

$$\boxed{\left(\int_a^b \hat{X}'\, K[\hat{X}]dt + \hat{S} \int_a^b \hat{X}'\, L[\hat{X}]dt \right) c = 0}$$

or, briefly

$$\boxed{(A + \hat{S}\, B)\, c = 0},$$

where A and B are matrices of q columns, and the designation $\hat{S}$ for the parameter indicates that we are here dealing with approximate values.

Nontrivial solutions of the equation system exist only if det $(A + \hat{S}\ B) = 0$. But since A and B are not singular with linear independent starting functions, /40 this yields a polynomial of the q^{th} degree in $\hat{S}$, the roots of which, $\hat{S}_1, \ldots, \hat{S}_q$, represent approximations to the desired eigenvalue S. For each $\hat{S}$ we obtain a set of constants $c_1, \ldots, c_q$, which are defined only up to a common factor, and which, inserted in $\hat{x}$ approximate the matching eigenfunction.

Galerkin's method can be applied quite analogously to the approximation of eigenvalues and eigenfunctions of a system of r differential equations of degree $\leq n$, with corresponding linear homogeneous boundary conditions. Let the differential equations be summarized in the expression

$$\boxed{K[x] + S\ L[x] = 0} \qquad \text{(A3.4)}$$

where x(t) is now the vector of the independent variables, $x' = (x_1, \ldots, x_r)$, and K and L indicate matrices of r columns, the elements of which, K_{ij} and L_{ij}, $j = 1, \ldots, r$, consist of operators of the form (A3.2). If the differential equations are linear and independent, then either det $K \neq 0$ or det $L \neq 0$.

Each of the variables x_i, $i = 1, \ldots, r$, is now approximated again by a linear combination of q linear independent functions $\hat{X}_{i1}, \ldots, \hat{X}_{iq}$ which meet the matching boundary conditions:

$$\boxed{\hat{x}_i = \hat{X}_{i.} c_{.i} = \sum_{k=1}^{q} \hat{X}_{ik}\, c_{ki}}$$

with $\hat{X}_{i.} = (\hat{X}_{i1}, \ldots, \hat{X}_{iq})$ and $c_{.i}' = (c_{1i}, \ldots, c_{qi})$ so that, corresponding to (A3.3), we can make up the formulation

$$\hat{x} = \begin{pmatrix} \hat{x}_1 \\ \vdots \\ \hat{x}_r \end{pmatrix} = \begin{pmatrix} \hat{X}_1, & 0, & \ldots, & 0 \\ \cdots & \cdots & \cdots & \cdots \\ 0 & 0, & \ldots, & \hat{X}_r \end{pmatrix} \begin{pmatrix} c_{.1} \\ \vdots \\ c_{.r} \end{pmatrix} = \hat{X}\, c \qquad \text{(A3.5)}$$

If we insert $\hat{x}$ into the system, we obtain the defect vector

$$K[\hat{x}] + S\, L[\hat{x}] = \Delta = (\Delta_1, \ldots, \Delta_r)' ,$$

and the Galerkin equations can be represented formally again as the matrix product /41

$$\left(\int_a^b \hat{X}' K[\hat{X}]dt + \hat{S} \int_a^b \hat{X}' L[\hat{X}]dt \right) c = 0$$

or

$$(\alpha + \hat{S}\beta)\, c = 0$$

with matrices α and β having rq columns. If the equation system is written out extensively, we obtain from the i^{th} differential equation in particular the q equations

$$\int_a^b \hat{x}_{i1} \left\{ K_{i1}\left[\sum_{k=1}^{q} \hat{x}_{1k}\, c_{k1} \right] + \ldots + K_{ir}\left[\sum_{k=1}^{q} \hat{x}_{rk}\, c_{kr} \right] \right\} dt +$$

$$\hat{S} \int_a^b \hat{x}_{i1} \left\{ L_{i1}\left[\sum_{k=1}^{q} \hat{x}_{1k}\, c_{k1} \right] + \ldots + L_{ir}\left[\sum_{k=1}^{q} \hat{x}_{rk}\, c_{kr} \right] \right\} dt = 0 ,$$

$$l = 1, 2, \ldots, q$$

But this means that the defect Δ_i in the interval [a,b] of the series is to be orthogonalized with respect to all the starting functions for x_i. Then every operator K_{ij} of the differential equation system contributes to the elements of a q-column submatrix A_{ij} of $\boldsymbol{\alpha}$. They can be calculated from

$$\int_a^b \hat{x}_{i1} K_{ij}[\hat{x}_{jk}]dt = (A_{ij})_{1k}.$$

The submatrices, which belong to one of the operators $K_{ij} \neq 0$ or $L_{ij} \neq 0$ are also not singular here, because the starting functions for each of the dependent variables x_i, i = 1, 2, ...r, are selected linear and independent. With independent differential equations, therefore, at least one of the matrices $\boldsymbol{\alpha}$, $\boldsymbol{\mathcal{L}}$ must be regular. The approximate values $\hat{S}_\nu, \nu = 1,2,\ldots,rq,$ for the desired eigenvalue S are the roots of the characteristic equation of the matrix $(-\boldsymbol{\mathcal{L}}^{-1}\boldsymbol{\alpha})$ or, in case det $\boldsymbol{\mathcal{L}}$ = 0, the reciprocal eigenvalue of $(-\boldsymbol{\alpha}^{-1}\boldsymbol{\mathcal{L}})$. /42
The set of rq constants belonging to $\hat{S}_\nu$ provides approximations for the eigenfunctions.

A4. The Numerical Solution

To solve the system (4.5) — i.e., to calculate the smallest eigenvalue S_1 and its eigenfunctions — the method of Galerkin is used. In the notation of Section 3 (with r = 3; x_1 = u; x_2 = v, x_3 = p) the differential Equations (4.5) are

$$\begin{aligned} K_{11}[u] + K_{12}[v] &= 0 \\ K_{22}[v] + K_{23}[p] + S\,L_{21}[u] &= 0 \\ K_{32}[v] + K_{33}[p] &= 0, \end{aligned}$$

with the operators $(D = \frac{d}{d\eta})$

$$K_{11} = M(D^2 - \sigma^2) + M'D \qquad K_{12} = -\bar{U}'$$
$$K_{22} = M(D^2 - \sigma^2) + 2M'D \qquad K_{23} = -D$$
$$K_{32} = M(D^3 - \sigma^2 D) + M'(D^2 + \sigma^2) \qquad K_{33} = -\sigma^2$$
$$L_{21} = -e^{-\gamma\eta}\bar{U}$$

and otherwise zero.

Following the ideas in Section 6, we select as the starting functions

$$\hat{u}_{1k} = (1 - e^{-\eta})^{n_{1k}} e^{-r_{1k}\eta}$$
$$\hat{v}_{2k} = (1 - e^{-\eta})^{n_{2k}} e^{-r_{2k}\eta}$$
$$\hat{p}_{3k} = (1 - e^{-\eta})^{n_{3k}} e^{-r_{3k}\eta}$$

in which $k = 1, 2, \ldots, q$; n_{ik} is greater than or equal to zero throughout; r_{ik} is greater than zero.

The boundary conditions $u = v = v' = 0$ at $\eta = 0$ and $\eta \to \infty$ as well as the relation $p(\infty) = 0$ which follows from (6.1.3) are fulfilled if the exponents are selected so that $n_{1k} \geq 1$, $n_{2k} \geq 2$, $n_{3k} \geq 0$. Furthermore, we must note that the starting functions are linear and independent with respect to each of the variables — that is, that for any two starting functions, the exponents of $(1 - e^{-\eta})$ or of $e^{-\eta}$ are different. /43

Now we set up the Galerkin equations $(\alpha + \hat{S}\gamma)\,o = 0$ by the method described in Section A3. That is, we introduce the approximations $\hat{u}$, $\hat{v}$, $\hat{p}$ into the differential equations and orthogonalize the first defect in the interval $(0, \infty)$ of the series according to all the starting functions $\hat{u}_{1k}$, the second to $\hat{v}_{2k}$, and the third to $\hat{p}_{3k}$. To calculate the elements of α and γ, we must evaluate integrals of the form

$$\int_0^\infty f(\eta)\,(1 - e^{-\eta})^n\, e^{-r\eta}\, d\eta$$

where $f(\eta)$ can be one of the coefficient functions $\bar{U}(\eta)$, $\bar{U}'(\eta)$, $M(\eta)$ and $M'(\eta)$. Because $\bar{U}'(\eta) = M'(\eta) \equiv 0$ for $\eta \geq 1$, the integration interval for the corresponding summands reduces from the first to the interval [0, 1]. Both of the other coefficient functions can be represented as $M(\eta) = 1 + \mathrm{Re}\, m(\eta)$ and $\bar{U}(\eta) = 1 + (\bar{U}(\eta) - 1)$ with $m(\eta) = \bar{U}(\eta) - 1 \equiv 0$ for $\eta \geq 1$, so that here again we can divide the integration into

$$\int_0^\infty (1 - e^{-\eta})^n e^{-r\eta}\, d\eta + \int_0^1 g(\eta)\, (1 - e^{-\eta})^n e^{-r\eta}\, d\eta$$

If we apply the already known polynomial (see A2) to describe the coefficient functions in the individual segments of [0, 1], we only have expressions which can be integrated analytically. That is, we have

$$\int_a^b \eta^t e^{-\sigma\eta}\, d\eta = \frac{t!}{s^{t+1}} \sum_{\tau=0}^{t} \left(e^{-sa} \frac{(sa)^\tau}{\tau!} - e^{-sb} \frac{(sb)^\tau}{\tau!} \right) . \qquad \text{(A4.1)}$$

To be sure, the complete analytical calculation of the finite portion of the integral leads to fourfold sums. Since the accuracy with which these sums can be evaluated still depends on the exponents n and r, and is otherwise very difficult to review, we have in most cases calculated the integrals numerically by Simpson's rule.

In comparison, integration over the infinite interval was done analytically: (A4.1) yields first

/44

$$\int_0^\infty \eta^t e^{-s\eta} d\eta = \frac{t!}{s^{t+1}} ,$$

and from that there follows

$$\int_0^\infty (1-e^{-\eta})^n e^{-r\eta}\, d\eta = \sum_{\nu=0}^{n} (-1)^\nu \binom{n}{\nu} \frac{1}{\nu + r} .$$

Corresponding to the operational notation of the differential equation system, we can divide the Galerkin equations $(\alpha + \hat{S}\mathcal{B})\,c = 0$ as follows:

$$\left[\begin{pmatrix} A_{11} & A_{12} & 0 \\ 0 & A_{22} & A_{23} \\ 0 & A_{32} & A_{33} \end{pmatrix} + \hat{S}\begin{pmatrix} 0 & 0 & 0 \\ B_{21} & 0 & 0 \\ 0 & 0 & 0 \end{pmatrix}\right]\begin{pmatrix} c_{.1} \\ c_{.2} \\ c_{.3} \end{pmatrix} = 0\,. \tag{A4.2}$$

By multiplication from the left with $\alpha^{-1}\ (\det\alpha \neq 0)$, we can reduce the eigenvalue problem of the matrix pair $\alpha, \mathcal{B}$ to

$$(\alpha^{-1}\mathcal{B} + \hat{S}^{-1}\mathcal{E})\,c = 0\,, \tag{A4.3}$$

and thus to the determination of the eigen-solutions of $-\alpha^{-1}\mathcal{B}$. Let us again consider the matrix α^{-1} to be analyzed into q-column submatrices X_{ij} which we can calculate on the basis of the relation $\alpha\alpha^{-1} = \mathcal{E}$ from the nine linear equations

$$\sum_{k=1}^{3} A_{ik}X_{kj} = E_{ij} \qquad i,j = 1,2,3$$

Because

$$\alpha^{-1}\mathcal{B} = \begin{pmatrix} X_{11} & X_{12} & X_{13} \\ X_{21} & X_{22} & X_{23} \\ X_{31} & X_{32} & X_{33} \end{pmatrix}\begin{pmatrix} 0 & 0 & 0 \\ B_{21} & 0 & 0 \\ 0 & 0 & 0 \end{pmatrix} = \begin{pmatrix} X_{12}B_{21} & 0 & 0 \\ X_{22}B_{21} & 0 & 0 \\ X_{32}B_{21} & 0 & 0 \end{pmatrix}$$

it is sufficient to know the submatrices $X_{12} = -A_{11}^{-1}A_{12}X_{22}$, $X_{22} = (A_{22} - A_{23}\cdot A_{33}^{-1}A_{32})^{-1}$ and $X_{32} = -A_{33}^{-1}A_{32}X_{22}$. /45

For the existence of a nontrivial solution vector of (A4.3), it is required that

$$\boxed{\left(\alpha^{-1}\mathfrak{B}+\hat{S}^{-1}\mathfrak{E}\right)=0}$$

This provides an algebraic equation of degree 3q for $\hat{S}^{-1}$. Due to the structure of $\mathfrak{H}$, the characteristic equation breaks up into

$$\boxed{\left(X_{12}B_{21}+\hat{S}^{-1}B_{11}\right)\hat{S}^{-2q}=0\,,}$$

with the 2q-fold zero point $\hat{S}^{-1}=0$. The remaining q eigenvalues of $\boxed{-\alpha^{-1}\mathfrak{B}}$ agree with those of $-X_{12}B_{21}$.

We calculate the greatest eigenvalue $\hat{S}_1^{-1}$, which corresponds to the desired smallest eigenvalue $\hat{S}_1$ of (A4.2), by the iteration method, iterating according to the rule

$$\boxed{c_{.1}^{(\nu+1)}=-X_{12}B_{21}\,c_{.1}^{(\nu)}\,.}$$

There the initial vector $c_{.1}^{(0)}$ must have one component of the eigenvector.

The calculation shows that the series of quotients of corresponding components of two successive vectors converges, approaching a simple positive eigenvalue. The normalized vectors themselves approach the matching eigenvector

$$\boxed{\frac{c_{i1}^{(\nu+1)}}{c_{i1}^{(\nu)}}\longrightarrow\hat{S}^{-1}\quad\text{and}\quad c_{.1}^{(\nu)}\longrightarrow c_{.1}\,.}$$

Using the eigenvectors $c_{.1}$ of $-X_{12}B_{21}$, we determine the eigenvector c for the eigenvalue $\hat{S}^{-1}$ of $\boxed{-\alpha^{-1}\mathfrak{B}}$ from

$$\boxed{\begin{pmatrix}-X_{12}B_{21} & 0 & 0\\ -X_{22}B_{21} & 0 & 0\\ -X_{32}B_{21} & 0 & 0\end{pmatrix}\begin{pmatrix}c_{.1}\\ 0\\ 0\end{pmatrix}-\begin{pmatrix}-X_{12}B_{21}\,c_{.1}\\ -X_{22}B_{21}\,c_{.1}\\ -X_{32}B_{21}\,c_{.1}\end{pmatrix}=\hat{S}^{-1}\begin{pmatrix}c_{.1}\\ c_{.2}\\ c_{.3}\end{pmatrix}\,.}$$

The vector c is simultaneously the eigenvector of (A4.2) for the eigenvalue $\hat{S}$, and the desired eigenfunctions are given by $\hat{u} = \hat{u}_{1,c_{,1}}$, $v = \hat{v}_{2,c_{,2}}$ and $\hat{p} = \hat{p}_{3,c_{,3}}$. /46

$\hat{S}_1^{-1}$ can be calculated with any desired accuracy as the eigenvalue from $-X_{12}B_{21}$ by the iteration method. The elements of this matrix are, to be sure, burdened with errors arising in the calculation of matrix X_{12} from submatrices of α. The effect of these errors on the magnitude of the eigenvalue can be estimated if we compare the results given in performing the calculation with the same starting functions but with a different sequence of the starting functions. But it is not possible to state how far the approximations diverge from the eigen-solutions of (4.5).

All the numerical computations were performed on the Siemens 2002 computer system in the Computer Center of the Institute for Applied Mathematics of the University, Freiburg.

8. SUMMARY

In this work it is shown that Taylor-Görtler longitudinal vortices can occur in a turbulent boundary layer at a concave wall if the curvature of the wall is large enough.

As in all such investigations, the theorem of vortex instability leads to an eigenvalue problem from which a critical curvature can be determined for neutral perturbations (and only these are considered here) at a prescribed basic flow and for any perturbation wavelength. For a complete description of the turbulent gasic flow, a profile of the turbulent apparent viscosity and the Reynolds number must be prescribed along with the velocity profile.

The eigenvalue problem is solved approximately by the Galerkin method for a turbulent boundary layer flow described by P. S. Klebanoff. The results

proved to be strongly dependent on the choice of the starting functions, but they agree within an order of magnitude. In each approximation, the critical curvature calculated for a given Reynolds number has a minimum value for a certain wavelength. It increases for larger and smaller values of the parameter, with increasing steepness. /47

Finally, the Reynolds number was varied within a certain range, on the assumption that a suitably plotted basic profile would not change. For the curves of critical curvature, this gives a slight shift to smaller values of curvature with increasing Reynolds number.

In conclusion, the experimental results determined by I. Tani are mentioned. The theoretical studies agree satisfactorily with them.

9. REFERENCES

/48

1. Schlichting, H. Grenzschicht-Theorie (Boundary Layer Theory). Verlag G. Braun, Karlsruhe (1958).

2. Görtler, H. On a Three-Dimensional Instability of Laminar Boundary Layers at Concave Walls. Ges. Wiss. Göttingen, Fachgruppe I, Neue Folge 2, 1940, pp. 1-27.

3. Taylor, G.I. Stability of a Viscous Liquid Contained Between Two Rotating Cylinders. Phil. Trans. Roy. Soc. London, Ser. A 223, 1923, pp. 289-343.

4. Hämmerlin, G. On the Eigenvalue Problem of the Three-Dimensional Instability of Laminar Boundary Layers at Concave Walls. Journ. Rat. Mech. Anal., Vol. 4, 1955, pp. 279-321.

5. Hämmerlin, G. On the Theory of Three-Dimensional Instability of Laminar Boundary Layers. A. Angew. Math. Phys., Vol. 7, 1956, pp. 156-164.

6. Smith, A. M. O. On the Growth of Taylor-Görtler Vortices Along Highly Concave Walls. Quart. Appl. Math., Vol. 13, 1955, pp. 233-262.

7. Hämmerlin, G. On the Stability of a Compressible Flow Along a Concave Wall at Different Wall Temperature Conditions. Bericht der Deutschen Versuchsanstalt für Luftfahrt, e.V., No. 176, 1961.

8. Becker, E. Hydrodynamics II. Lecture, Winter Semester, 1961-62, Freiburg i. Br., Chapter IV, Section 2 and Chapter V, Section 9.

9. Reynolds, O. On the Dynamic Theory of Incompressible Viscous Fluids and the Determination of the Criterion. Phil. Trans. Roy. Soc. London, Ser. A 186, 1895, pp. 123-164.

10. Boussinesq, I. Théorie de l'écoulement tourbillant (Theory of Turbulent Flow), Paris 1897.

11. Prandtl, L. The Mechanics of Viscous Fluids. Handbook article from W.F. Durand: Aerodynamic Theory, Division G., Vol. III, pp. 34-208, J. Springer, Berlin 1935.

12. Görtler, H. Effect of Slight Waviness in the Wall on the Course of the Laminar Boundary Layers. Z. Angew. Math. Mech., Vols. 25-27, 1947 pp. 233-244.

13. Witting, H. On the Effect of Flow Line Curvature on the Stability of Laminar Flows. Arch. Rat. Mech. Anal., Vol. 2, 1958, pp. 243-283. /49

14. Di Prima, R.C. Application of the Galerkin Method to Problems in Hydrodynamic Stability. Quart. Appl. Math., Vol. 13, 1955, pp. 55-62.

15. Di Prima, R.C. and D.W. Dunn. The Effect of Heating and Cooling on the Stability of the Boundary Layer Flow of a Liquid Over a Curved Surface. Journ. Aeron. Sci., Vol. 23, 1956, pp. 913-916.

16. Frazer, R.A., W.J. Duncan and A.R. Collar. Elementary Matrices. Art. 7.9, University Press, Cambridge 1950, pp. 224-228.

17. Duncan, W.J. Galerkin's Method in Mechanics and Differential Equations. Aeronautical Research Committee Reports and Memoranda, No. 1798, London 1937.

18. Klebanoff, P.S. Characteristics of Turbulence in a Boundary Layer with Zero Pressure Gradient. National Advisory Committee for Aeronautics, Technical Note No. 3178, Washington, July 1954.

19. Nikuradse, J. Turbulent Friction Layers at a Plate. Herausgegeb. Zentr. wiss. Ber.-Wesen. In Komm. bei R. Oldenbourg, München und Berlin 1942.

20. Nikuradse, J. Regularity of Turbulent Flow in Smooth Tubes. Forschungs-Arb. Ing. Wesen, Heft 356, 1932.

21. Tani, I. Production of Longitudinal Vortices in the Boundary Layer Along a Concave Wall. Journ. of Geophysical Research, Vol. 67, No. 8, 1962, pp. 3075-3080.

22. Clauser, F.H. The Turbulent Boundary Layer. Advances in Applied Mechanics IV (herausgegeben von R. V. Mises und Th. V. Kármán) Academic Press Inc., pp. 1-51.

Translated for National Aeronautics and Space Administration under Contract No. NASw 2035, by SCITRAN, P.O. Box 5456, Santa Barbara, California, 93108.